Nano Biomed Eng
2019, 11(1): 18-27. doi: 10.5101/nbe.v11i1.p18-27.

Research Article

Polyethylene Glycol-Functionalized Magnetic (Fe_3O_4) Nanoparticles: A Novel DNA-Mediated Antibacterial Agent

Majid Sakhi Jabir[1], Uday Muhsen Nayef[2], Waleed Kamel Abdul Kadhim[2]

[1]Division of Biotechnology, Department of Applied Science, University of Technology, Baghdad, Iraq.
[2]Division of Applied Physics, Department of Applied Science, University of Technology, Baghdad, Iraq.

Corresponding authors. E-mail: msj_iraq@yahoo.com;unayef@yahoo.com

Received: May 14, 2018; **Accepted:** Sep. 25, 2018; **Published:** Feb. 22, 2019.

Citation: Majid Sakhi Jabir, Uday Muhsen Nayef, and Waleed Kamel Abdul Kadhim, Polyethylene Glycol-Functionalized Magnetic (Fe_3O_4) Nanoparticles: A Novel DNA-Mediated Antibacterial Agent. *Nano Biomed. Eng.*, 2019, 11(1): 18-27.
DOI: 10.5101/nbe.v11i1.p18-27.

Abstract

The Fe_3O_4-PEG magnetic nanoparticles (NPs) were prepared by hydrothermal method at different concentrations ($FeCl_3{\cdot}6H_2O$ 0.75 mg/mL and $FeCl_3{\cdot}6H_2O$ 1.5 mg/mL) and subsequently surface-functionalized coating with polyethylene glycol (PEG), the successful coating of PEG molecules on the surface of Fe_3O_4. These magnetic NPs exhibited good dispersibility and dissolvability in physiological condition. The obtained magnetic nanoparticles were characterized by X-ray diffraction (XRD), transmission electron microscopy (TEM), Fourier transform infrared (FTIR) spectroscopy, thermogravimetry (TG) and vibrating sample magnetometer (VSM). The antibacterial activity of Fe_3O_4-PEG magnetic nanoparticles (MNPs) was studied against two bacterial strains: Gram-positive *Staphylococcus and* Gram-negative *Escherichia coli* aureus. The modified MNPs had a significant effect is more on *S. aureus* and less on *E. coli*. The results showed that polyethylene glycol-functionalized magnetic (Fe_3O_4) NPs as a novel DNA-mediated antibacterial agent.

Keywords: Fe_3O_4-PEG, Antibacterial activity; Hydrothermal synthesis; DNA damage

Introduction

Nanoparticles (NPs) are submicron moieties (diameters ranging from 1 to 100 nm according to the used term, although there are examples of NPs several hundreds of nanometers in size) made of inorganic or organic materials, which have many novel properties compared with the bulk materials [1]. On this basis, magnetic NPs have many unique magnetic properties such as superparamagnetic, high coercivity, low Curie temperature, high magnetic susceptibility, etc. Magnetic NPs are of great interest for researchers from a broad range of disciplines, including magnetic fluids, data storage, catalysis, and bioapplications [2-6]. Especially, magnetic ferrofluids and data storage are the applied researches that have led to the integration of magnetic NPs in a myriad of commercial applications. Currently, magnetic NPs are also used in important bioapplications, including magnetic bioseparation and detection of biological entities (cell, protein, nucleic acids, enzyme, bacterials, virus, etc.), clinic diagnosis and therapy (such as magnetic resonance image (MRI)) andmagnetic fluid hyperthermia (MFH), targeteddrug delivery and biological labels, etc.

However, it is crucial to choose the materials for the construction of nanostructure materials and devices with adjustable physical and chemical properties. To this end, magnetic iron oxide NPs have become the strong candidates, and the application of small iron oxide NPs in in-vitro diagnostics has been practiced for nearly half a century [7]. In the last decade, increased investigations with several types of iron oxides have been carried out in the field of magnetic NPs (mostlyincluding the Fe_3O_4 magnetite, $Fe^{II}Fe^{III}{}_2O_4$, ferrimagnetic, superparamagnetic when the size is less than 15 nm), α-Fe_2O_3 (hematite, weakly ferromagnetic or antiferromagnetic), and γ-Fe_2O_3 (maghemite, ferrimagnetic) [8], among which magnetite and maghemite are the very promising and popular candidates giventheir biocompatibility that has already been proven. The iron oxide NPs with controlled size and shape are technologically important due to the strong correlation between these parameters and magnetic properties. The microemulsion and thermal decomposition methods usually lead to complicated process or require relatively high temperatures. As an alternative, hydrothermal synthesis includes various wet chemical technologies of crystallizing substance in a sealed container from the high temperature aqueous solution (generally in the range from 130 to 250 °C) at high vapour pressure (generally in the range from 0.3 to 4 MPa). This technique has also been used to grow dislocation-free single crystal particles, and grains formed in this process could have a better crystallinity than those from others, so hydrothermal synthesis is prone to obtain the highly crystalline iron oxide NPs.Although most studies have focused on the development of small organic molecules and surfactants coating up to now, recently polymers functionalized iron oxide NPs are receiving more and more attention, owing to the fact that advantages of polymers coating will increase repulsive forces to balance the magnetic and the van der Waals attractive forces acting on the NPs.

In addition, polymers coating onthe surface of iron oxide NPs offer a high potential in the application of several fields. Moreover, polymer functionalized iron oxide NPs have been extensively investigated due to the interest in their unique physical or chemical properties. Polymer coating materials can be classified into synthetic and natural. The saturation magnetization value of iron oxide NPs will decrease after polymers functionalization. Currently, there are two major developing directions to form polymers functionalized iron oxide NPs. One is for the purpose of expanding the application range by introducing functional polymers. For instance, Gupta et al. [9] reported a microemulsion polymerization process to prepare polyethylene glycol (PEG)-modified superparamagnetic iron oxide NPs with magnetic core and hydrophilic polymeric shell. Highly monodispersed iron oxide NPs were synthesized by using the aqueous core of aerosol-OT (AOT)/n-Hexane reverse micelles (without microemulsions) in N_2 atmosphere. The average size of the PEG-modified NPs was found to be around 40-50 nm with narrow size distribution. It is important that the cytotoxicity profile of the NPs on human dermal fibroblasts, as measured by standard 3-(4,5-dimethylthiazol-2-yl)-2,5-diphenyltetrazolium bromide assay, showed that the particles are nontoxic and may be useful for various in-vivo and in-vitro biomedical applications. Another is for the purpose of manufacturing monodisperse NPs with a well-defined shape and controlled composition [10].

Experimental

Chemicals and materials

Ferric chloride hexahydrate ($FeCl_3 \cdot 6H_2O$), anhydrous sodium acetate (NaOAc), polyethylene glycol (PEG)-4000, ethylene glycol (EG), ethanolamine (ETA) and ethanol were purchased from Beijing Chemicals (Beijing, China). Calcein AM was obtained from Sigma-Aldrich (Shanghai, China). All chemical agents were of analytical grade and used directly without further purification.

Preparation of Fe_3O_4-PEGmagnetic nanoparticles (MNPs)

Fe_3O_4-PEG MNPs were synthesis by hydrothermal method. $FeCl_3 \cdot 6H_2O$ (0.75 mg/dL and 1.5 mg/mL) was dissolved in solvent containing equal volume of EG and ETA. NaOAc (4 g) and PEG-4000 (2 g) were added into the above solution under magnetic stirring. The homogeneous solution was transferred to a Teflon-lined stainless-steel autoclave (100 mL) and sealed to heat at 200 °C. After reaction for 10 h, the autoclave was cooled to ambient temperature naturally. The MNPs were washed with ethanol and deionized water (DW) in sequence, and then dried in vacuum at 60 °C overnight.

Characterization of MNPs

The prepared MNPs were identified by structural

and optical techniques. X-ray diffraction (XRD) characterizations of the synthesized MNPs was made by powder using a Shimadzu XRD 6000 with Cu-Kα radiation source at 2θ =10°- 80°. An 8000 Series Shimadzu Fourier transform infrared spectroscopy (FTIR) system was used to study the molecular vibrations of the prepared samples. To examine the morphological properties of the MNPs, transmission electron microscopy (TEM; Philips) was used. Samples for TEM analysis were prepared by providing a MNPs solution drop on a Cu grid coated with gold (containing about 200 meshes). The magnetic properties were measured on a BHV-55 vibrating sample magnetometer (VSM). PerkinElmer TGA-7 was employed to perform the thermogravimetric analysis (TGA). Dried sample was placed in the TGA furnace and the measurements were carried out under nitrogen with a heating rate of 20 °C/min from 25 to 600 °C.

Antibacterial activity

Agar well diffusion assay

In this study, the antibacterial activity of Fe_3O_4-PEG magnetic NPs was investigated against two types of bacterial strains: *E. coli* and *S. aureus* using agar well diffusion assay. About 20 mL of Mueller-Hinton (M-H) was aseptically poured into sterile Petri dishes before culturing. The bacterial species were collected from their stock cultures using a sterile wire loop. After culturing the organisms, 6 mm-diameter wells were bored on the agar plates using of a sterile tip. Into the bored wells, different concentrations of the bare Fe_3O_4 and Fe_3O_4-PEGNPs (100, 250 and 500 µg/mL) were used. The cultured plates containing the NPs and the test organisms were incubated overnight at 37 °C before measuring and recording the average diameter of the produced zones of bacterial inhibition by the respective nanoparticle concentrations. The experiments were performed in triplicate. DW was used as a negative control.

Release of cellular materials

This method was done using sterile peptone water (0.75 g/50 mL) that was sterilizedat 15l bs pressure and 121°C temperature in 15 min. Then the medium inoculated with each bacterial strain. After 24 h in incubation, the prepared solutions of Fe_3O_4-PEG MNPs at concentration of 100 µg/mL was put into each tube. After 0, 30, 60 and 120 min of treatment, cells were centrifuged at 3500 rpm, and the absorbance of spectrum was determined at 510 nm. Results were expressed as the percentage between the absorbing materials in 510 nm of each interval with the time [12].

Detection of reaction oxygen species (ROS)

An acridine orange/ethidium bromide (AO/EB) staining procedure was used to detect the release of ROS by the treated and non-treated bacterial cells. For the antibacterial activity of the NPs on the studied organisms, a fluorescent microscope was used. Cell viability after treatment was distinguished using AO/EB staining procedure. 50 µL of the treated and non-treated bacterial suspension was mixed with 50 µL of 10 µg/mL AO/EB and allowed for 5 min. After staining, a film of the mixture was made on a glass slide and immediately examined under an immunofluorescent microscope. With this staining procedure, the acridine orange-stained living cells fluoresced green while the ethidium bromide-stained dead cells fluoresced red [13].

Electrophoresis analysis of DNA fragmentation

Analysis of DNA fragmentation was performed using bacterial extraction kit according to manufacturer's protocol. Bacterial strains were treated with Fe_3O_4-PEG at different concentrations ($FeCl_3 \cdot 6H_2O$ 0.75 mg/mL, and $FeCl_3 \cdot 6H_2O$ 1.5 mg/mL). For the treated and untreated bacterial strains, the DNA cells suspension was centrifuged (10000 rpm) at 4 °C for 10 min. The DNA was dissolved with DNA loading buffer, and then applied to 1.5% agarose gel electrophoresis. UV illuminator was used to visualize the results.

Statistical analysis

The comparison between groups was made using unpaired t-test. A p-value of <0.05 was considered significant [14].

Results and Discussion

Structural properties of Fe_3O_4-PEG MNPs

The XRD patterns of both prepared samples are shown Fig. 1. The prepared samples were composed of crystalline single phase cubic inverse spinal Fe_3O_4 structure, where the position and relative intensity of all observed diffraction peaks matched well with those of the JCPDS card number (11-0614) for magnetite. No peak was observed from any impurities. The characteristic peaks of the coated NPs had no shifting in the position but presented some broadening, indicating that the Fe_3O_4-PEG MNPs had small crystalline size as compared with Fe_3O_4-PEG MNPs

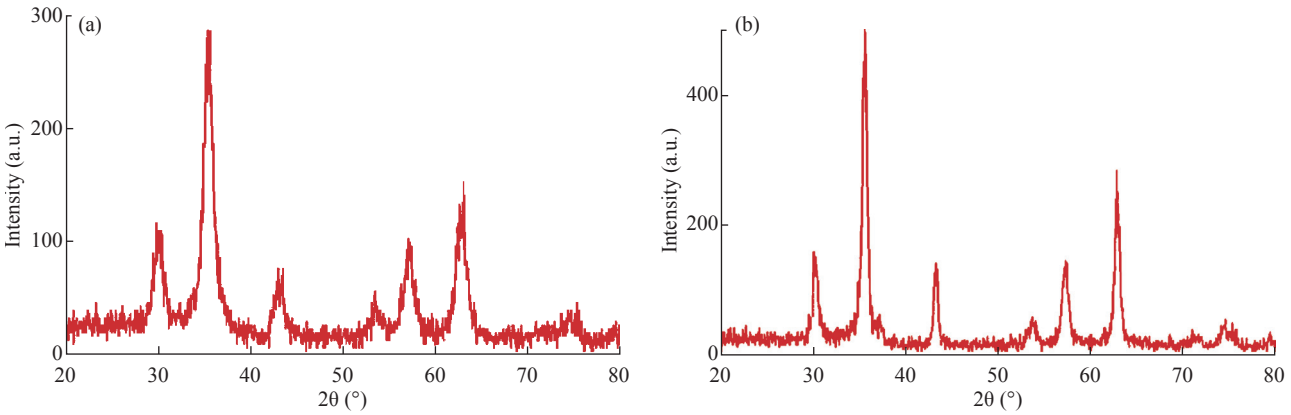


Fig. 1 XRD pattern of Fe_3O_4-PEG magnetic nanoparticles at different concentrations: **(a)** Fe_3O_4-PEG prepared using low concentration of $FeCl_3{\cdot}6H_2O$; and **(b)** Fe_3O_4-PEG magnetic nanoparticles prepared using high concentration of $FeCl_3{\cdot}6H_2O$.

prepared using high concentration of $FeCl_3{\cdot}6H_2O$. Furthermore, the peak intensity of the Fe_3O_4-PEG MNPs prepared using low concentration of $FeCl_3{\cdot}6H_2O$ was lower than the Fe_3O_4-PEG MNPs prepared using high concentration of $FeCl_3{\cdot}6H_2O$, which was related to the existence of PEG more coated on the surface of MNPs prepared in the previous way. The crystalline size was calculated by measuring the half-height width of the strongest reflection plane (i.e, 311), using the well-known Scherrer's relation ($D=0.9\ \lambda/\beta\ \cos(\theta)$), where, ($\beta$) is the full width at half maxima (FWHM) of the 311 peak. The calculations reveal ed that the Fe_3O_4-PEG MNPs prepared using low concentration of $FeCl_3{\cdot}6H_2O$ and Fe_3O_4-PEG MNPs prepared using high concentration of $FeCl_3{\cdot}6H_2O$ had sizes of 7.3 nm and 13.7 nm respectively [15].

Morphological properties of Fe_3O_4-PEG MNPs

For the better observation of morphology of the prepared MNPs, the TEM observation of samples are show in Fig. 2. It is clearly observable that both prepared MNPs had spherical shape. The Fe_3O_4-PEG MNPs prepared by using low concentration of $FeCl_3{\cdot}6H_2O$ exhibit ed better dispersibility as shown in Fig. 2(a), whereas the Fe_3O_4-PEG MNPs prepared using high concentration of $FeCl_3{\cdot}6H_2O$ were rather agglomerated. The less agglomerated texture may be related to the effect of polymer layer during the particle formation. The coating of Fe_3O_4 NPs with polymer led to decrease in the magnetic interaction among the particles due to their reduce magnetism and prevented their agglomeration [16]. From the TEM image, the mean diameters of MNPs were estimated to be 3 nm and 9 nm, respectively.

Chemical properties of Fe_3O_4-PEG MNPs

The surface chemical structures of Fe_3O_4-PEG-NPs were characterizd by Fourier-transform infrared (FTIR) spectroscopy. Fig. 3 exhibits the FTIR spectra of the PEG coated NPs. The broad peak near 3433-3446 cm^{-1} in all FTIR spectra belonged to the attached hydroxyl groups. Two broad peak bands around 628 and 584 cm^{-1} resulted from split of the ν_1 band of the Fe-O bond. The relative sharp band at 443 cm^{-1} corresponded to ν_2 band of the Fe-O bond. These results confirmed the magnetite phase of the prepared NPs after coating

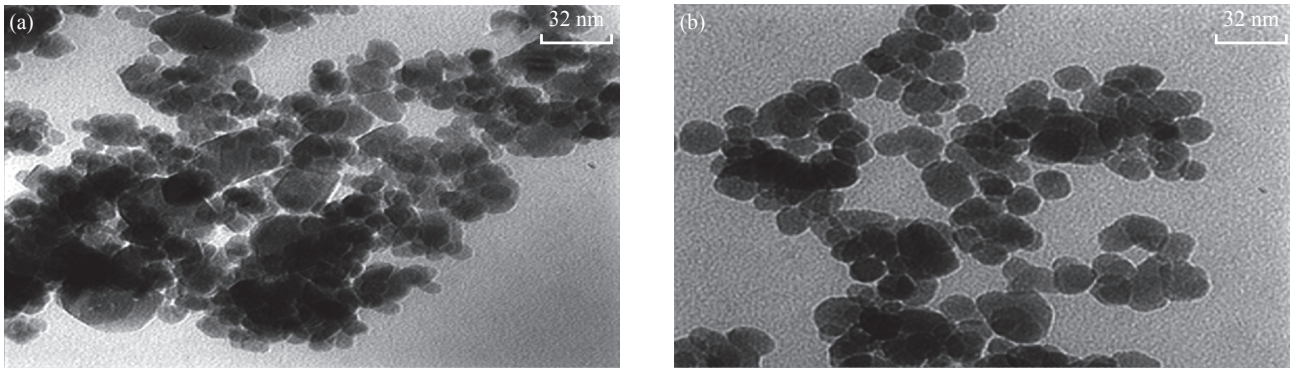


Fig. 2 TEM images of Fe_3O_4-PEG magnetic nanoparticles: **(a)** Fe_3O_4-PEG prepared using low concentration of $FeCl_3{\cdot}6H_2O$; and **(b)** Fe_3O_4-PEG magnetic nanoparticles prepared using high concentration of $FeCl_3{\cdot}6H_3O$.

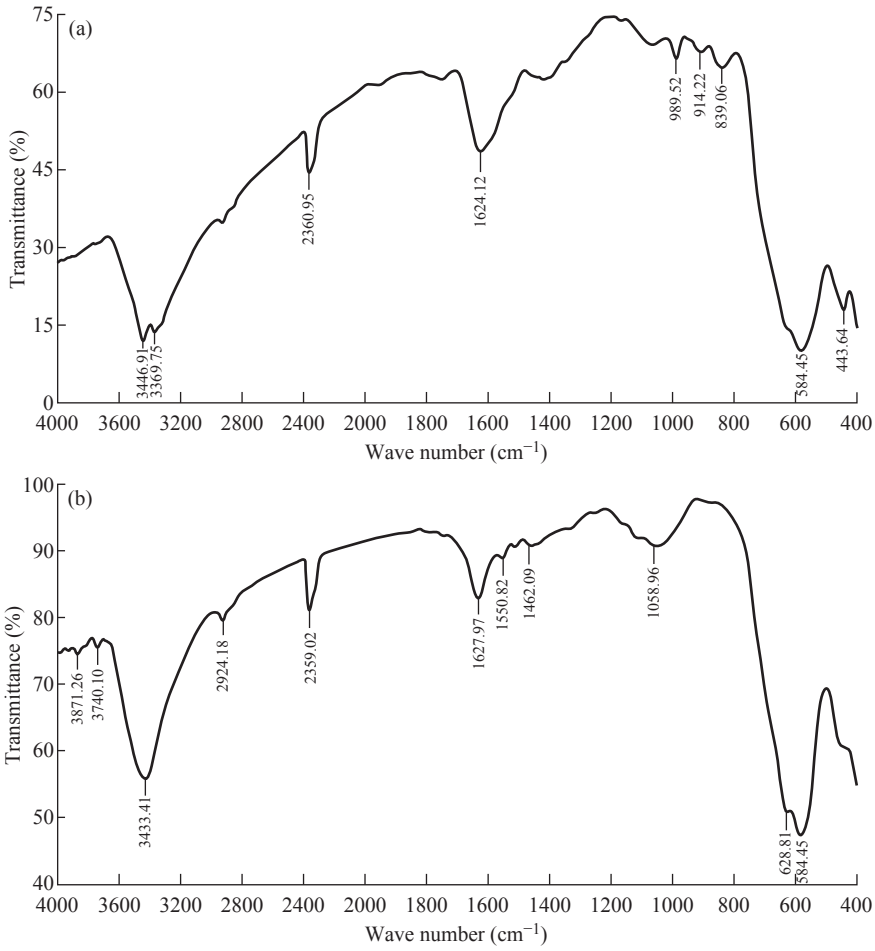


Fig. 3 FTIR spectra of Fe_3O_4-PEG magnetic nanoparticles: **(a)** Fe_3O_4-PEG prepared using low concentration of $FeCl_3{\cdot}6H_2O$; and **(b)** Fe_3O_4-PEG magnetic nanoparticles prepared using high concentration of $FeCl_3{\cdot}6H_2O$.

with PEG. The absorption bands around 1624-1627 cm^{-1} originated from stretching and deformation vibration hydroxyl groups connected to the surface of NPs. Also, the C-O-C ether stretch and vibration bands existed at 989 and 1058 cm^{-1}, respectively. The bands around 2924 and 916 cm^{-1} corresponded to the -CH stretching vibration and its out-of-plane bending vibration, respectively. The -CH-groups bending were also observed at 1462 cm^{-1}. These findings on FTIR spectra completely confirmed the PEG coat on the MNPs surface [17].

Vibrating sample magnetometer (VSM) of Fe_3O_4-PEG MNPs

Magnetic properties of the NPs were analyzed by use of the vibrating sample magnetometry at room temperature. Fig. 4 shows the hysteresis loops of the samples. The saturation magnetization was found to be 57.93 emu/g for Fe_3O_4-PEG MNPs prepared using low concentration of $FeCl_3{\cdot}6H_2O$, which waslower than the Fe_3O_4-PEG MNPs prepared by using high concentration of $FeCl_3{\cdot}6H_2O$ that was 59.66 emu/g. This difference suggested that large amount of polymer (PEG) encapsulated more ofMNPs prepared by low concentration than those prepared with high concentration. In addition; there was no hysteresis in the magnetization, with both remanence and coercively being zero, suggesting that these magnetic NPs were superparamagnetic [18]. When the external magnetic field was removed, the MNPs could be well dispersed by gentle shaking. These magnetic properties are potential for applications in both biomedical and bioengineering fields.

Thermogravimetric analysis (TGA) of Fe_3O_4-PEG MNPs

The thermo gravimetric analysis is one of the most important techniques and is used to determine thermal stability and physicochemical properties of compound by percent weight loss. Fig. 5 illustrates the TGA curve, explaining the variation of the remaining mass of the samples with temperature. The organic materials and magnetite of the samples were completely burned to generate gas products and converted into iron oxides at the increasing temperature, respectively.

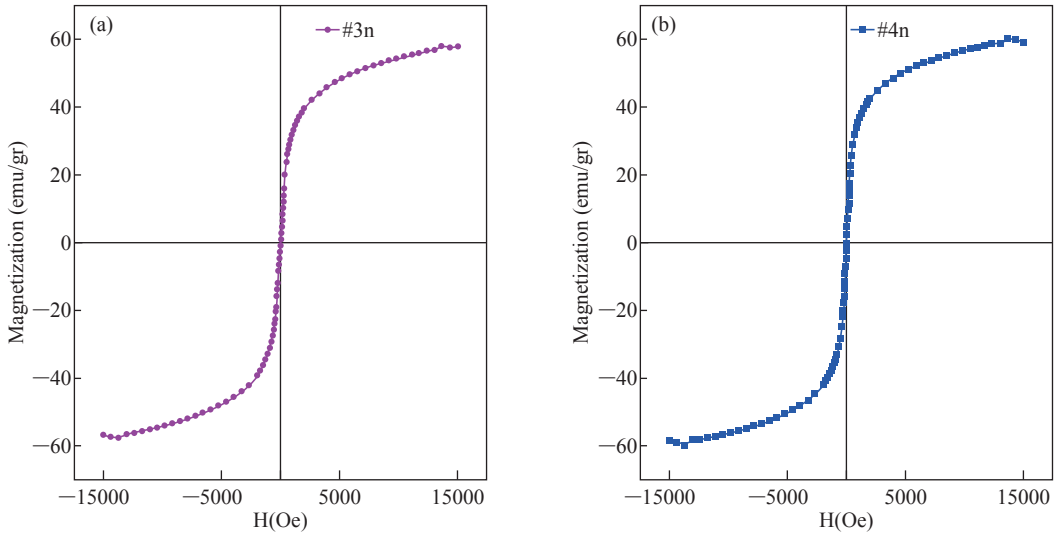


Fig. 4 VSM properties of Fe_3O_4-PEG magnetic nanoparticles: **(a)** Fe_3O_4-PEG prepared using low concentration of $FeCl_3 \cdot 6H_2O$; and **(b)** Fe_3O_4-PEG magnetic nanoparticles prepared using high concentration of $FeCl_3 \cdot 6H_2O$.

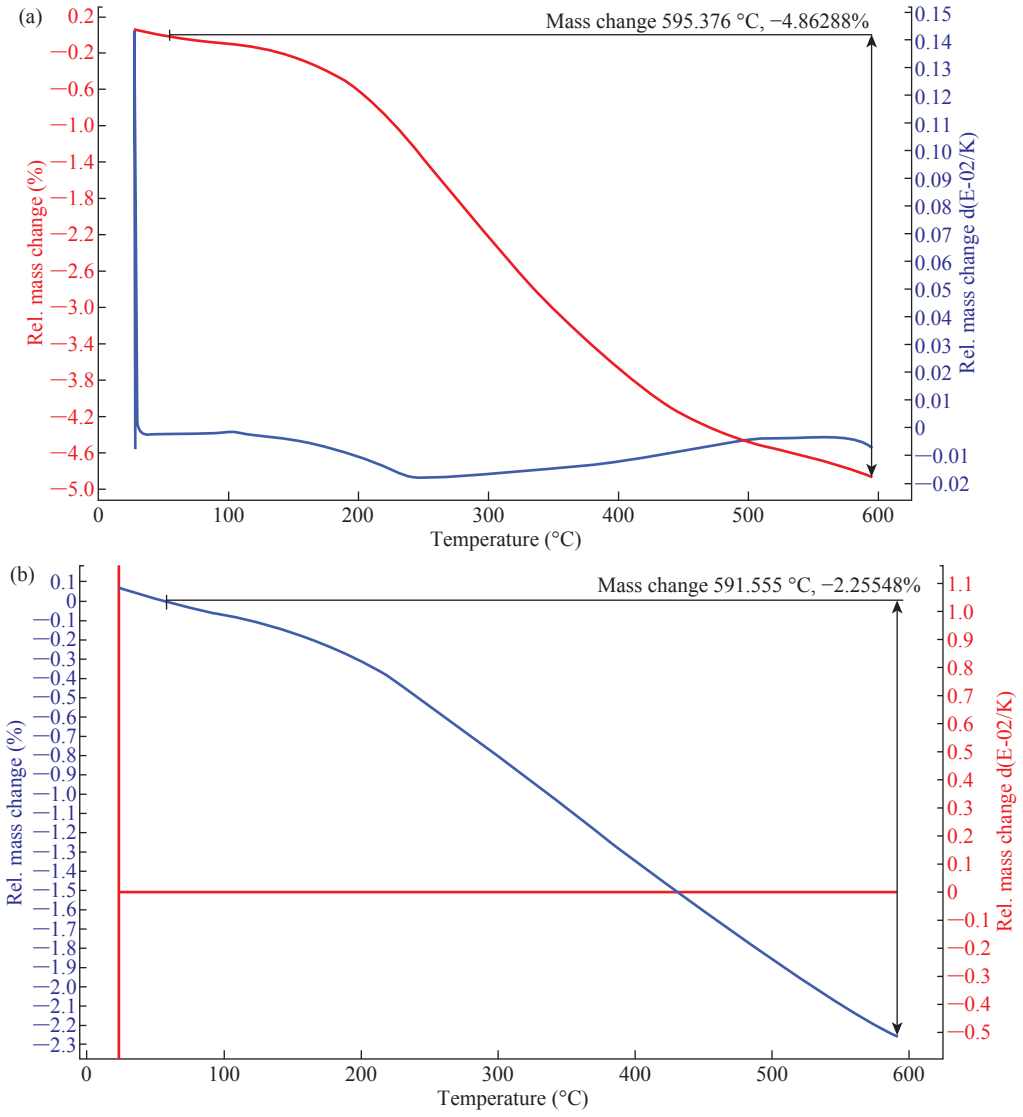


Fig. 5 Thermo gravimetric analysis Fe_3O_4-PEG magnetic nanoparticles: **(a)** Fe_3O_4-PEG prepared using low concentration of $FeCl_3 \cdot 6H_2O$; and **(b)** Fe_3O_4-PEG magnetic nanoparticles prepared using high concentration of $FeCl_3 \cdot 6H_2O$.

The first weight loss stage at 60 °C could be ascribed to the evaporation of water molecules in the polymer matrix, while the other stage beginning at about 220 °C was due to the decomposition of PEG. This change in profile of the thermogravimetry (TG) curve implicated that PEG molecules were chemically bond on the surface of Fe_3O_4 and not physically adsorbed. The PEG coated MNPs with high molecular weight of PEG would have the small percentage of the remainig mass [19]. The mass loss of about 4.86% was found for NPs prepared with low concentration and 2.25% was found for NPs prepared with high concentration of $FeCl_3{\cdot}6H_2O$, attributed to the decomposition of PEG.

Antibacterial activity of Fe_3O_4-PEG

In the present study, two standard bacterial strains,*S. aureus* and *E. coli*, were used. The zones of inhibition after exposing the organisms to different concentrations of Fe_3O_4-PEGwere measured and presented in Fig. 6. From the results, PEG-Fe_3O_4 prepared with low concentration of $FeCl_3{\cdot}6H_2O$ was found to be more effective on the bacterial growth than the Fe_3O_4-PEGprepared with high concentration of $FeCl_3{\cdot}6H_2O$. Effect of the NPs on the studied organisms was of a concentration-dependent manner. The resistance of microorganisms to external agentsis was due to the presence of an outer membranein the bacterial structure. PEG is a commonly selected coating material for many biomedical applications, such as to enhance the plasma half-life of MNPs in the bloodstream, to improve cellular uptake of NPs, and to avoid NPs aggregation. The absorbance of cellular materials secreted by the treated organisms at 220 nm is shown in Fig. 7. This method related optical density (OD) of the culture media at 220 nm to the time. As shown in Fig. 7, Fe_3O_4-PEGprepared with low concentration of $FeCl_3{\cdot}6H_2O$ exhibited a higher capacity of causing damage to the cell membrane of the studied organisms compared to those prepared with high concentration of $FeCl_3{\cdot}6H_2O$. The results indicated that Fe_3O_4-PEGcaused an increased permeability of the bacterial cytoplasmic membrane. It should be noted that the cytoplasmic membrane of bacteria served as a barrier to the leakage of ions [22, 23]. A recent study demonstrated that Linalool coated with gold NPs had great potential as antimicrobial activity

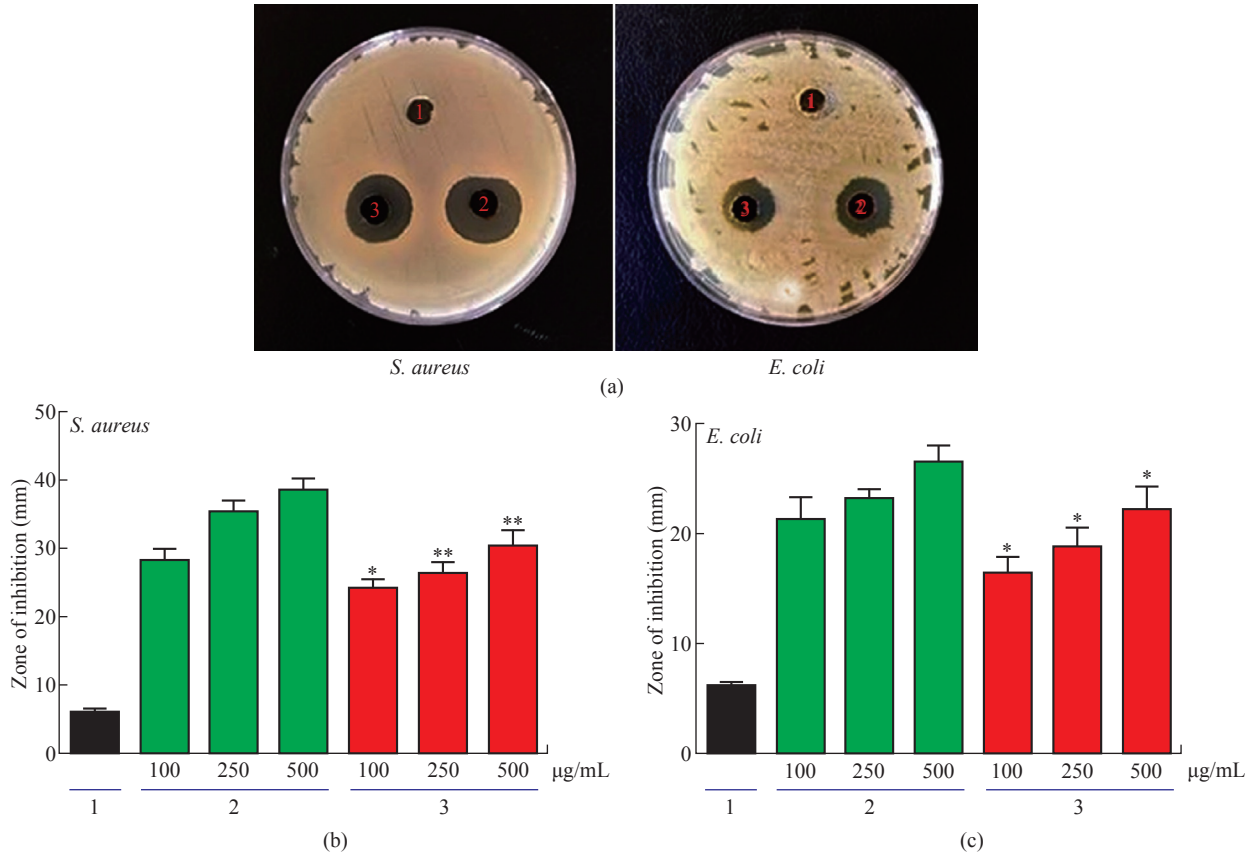


Fig. 6 Antibacterial activity of PEG-Fe_3O_4 magnetic nanoparticles against *S. aurues* and *E. coli.*: **(a)** Negative control; **(b)** Fe_3O_4-PEG prepared using low concentration of $FeCl_3{\cdot}6H_2O$; and **(c)** Fe_3O_4-PEG magnetic nanoparticles prepared using high concentration of $FeCl_3{\cdot}6H_2O$. The value are shown as the mean ± SD. *$p < 0.05$, **$p < 0.01$, and ***$p < 0.001$.

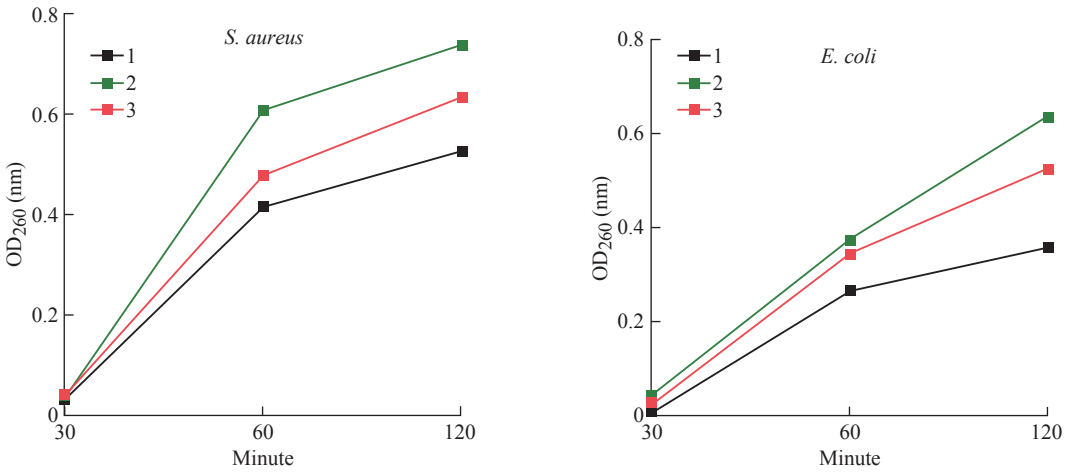


Fig. 7 Effects of PEG-Fe_3O_4 magnetic nanoparticles in bacterial cellular materials release: **(a)** Negative control; **(b)** Fe_3O_3-PEG prepared using low concentration of $FeCl_3 \cdot 6H_2O$; and **(c)** Fe_3O_4-PEG magnetic nanoparticles prepared using high concentration of $FeCl_3 \cdot 6H_2O$.

against bacterial strains such as *Staphylococcus and Escherichia coli* [24]. Another study showed the ability of carbon NPs decorated with cupric oxide in reduction of bacterial growth [25].

Detection of reaction oxygen species (ROS)

The changes in ROS production after bacterial strains being treated with Fe_3O_4-PEG were measured by using the fluorescence dye, AO/EB, which detected both hydrogen peroxide and nitric oxide that were considered as ROS indicator. Thus, in order to study the ROS production, the bacterial culture was inoculated with AO/EB dye which got oxidized with ROS production. Impact of the tested compounds on the viability of *E. coli* and *S. aureus* strains was studied by using fluorescent microscope. EB permeated only cells which lost membrane integrity and linked with nucleic acid. Viable cells appeared as green in colour and non-viable cells with nucleic acid damage appeared red in colour [26, 27]. The results showed Fe_3O_4-PEG NPs treated bacterial strains exhibited moderate effect on bacterial cell as compared with untreated *E. coli* and *S. aureus* cells as displayed in Fig. 8. Fe_3O_4-PEG NPs showed high activity to effect on the cell wall membrane of bacterial strains; most of the cells exhibited red in colour due to the loss

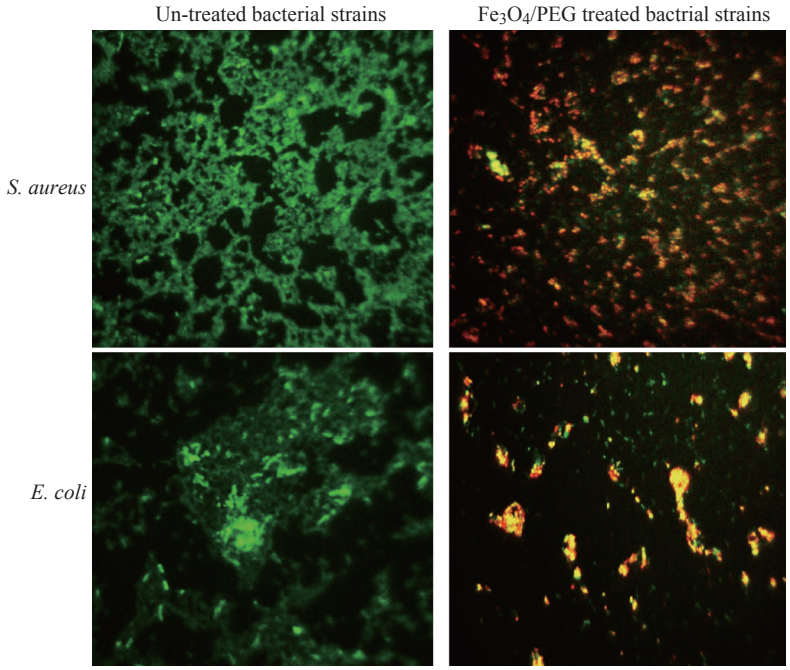


Fig. 8 Fluorescence microscopic images of the green and red fluorescence stained *S. aureus* and *E. coli* in absence and presence of PEG-Fe_3O_4 magnetic nanoparticles.

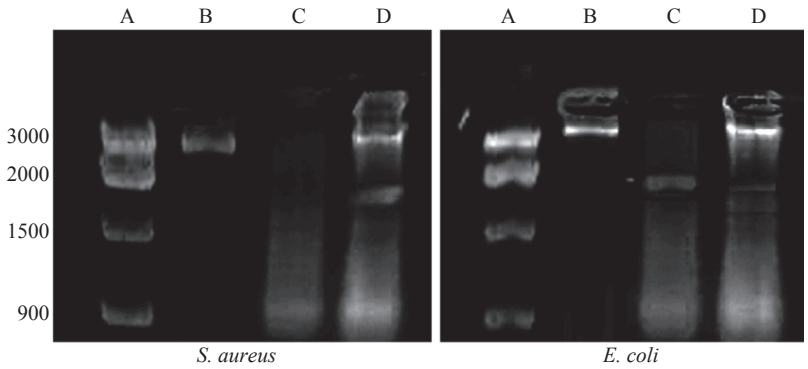


Fig. 9 Bacterial DNA fragmentation. Gel electrophoresis of bacterial strains treated and untreated as indicated: **(a)** DNA ladder; **(b)** Control untreated bacterial strains; **(c)** Bacterial strains treated with Fe_3O_4-PEG at the concentration of 1.5 mg/mL of $FeCl_3{\cdot}6H_2O$; and **(d)** Bacterial strains treated with Fe_3O_4-PEG at the concentration of 0.75 mg/mL of $FeCl_3{\cdot}6H_2O$.

of membrane integrity and interaction with damage nucleic acid as seen in Fig. 8. The results showed the prospective suitability of the studied Fe_3O_4-PEGNPs as antibacterial agents for future biological and biomedical applications.

Bacterial DNA fragmentation

To confirm the antibacterial activit of Fe_3O_4-PEG NPs, DNA-mediated, analysis of DNA fragmentation was done according to manufacturer's protocol. Fig. 9 represents a DNA fragmentation in bacterial strains after being treated with Fe_3O_4-PEG at different concentrations ($FeCl_3{\cdot}6H_2O$ 0.75 mg/mL and $FeCl_3{\cdot}6H_2O$ 1.5 mg/mL). DNA fragmentation was not observed in non-treated bacterial strains (control). On the other hand, in Fe_3O_4-PEG treated bacterial strains, the DNA fragmentation was very clear which suggested that Fe_3O_4-PEG at different concentrationswere able to kill bacterial strains via inducing fragmentation of bacterial DNA. Results of the present study revealed the antibacterial activity ofFe_3O_4-PEG at different concentrations was demonstrated by the DNA fragmentation assay. Furthermore, the results clearly showed that Fe_3O_4-PEG at different concentrations interacted with the DNA and made some structural or conformational changes which could alter the metabolic function and cause damage of bacterial cellular components.

Conclusions

The Fe_3O_4-PEG MNPs were prepared by hydrothermal method and characterized by XRD, TGA, FTIR, TEM and VSM. The surface modifying of MNPs with PEG provided stability and enhanced biocompatibility for MNPs. The results confirmed that the prepared MNPs had proper physicochemical and magnetic properties for antimicrobial applications.

Conflict of Interests

The authors declare that no competing interest exists.

References

[1] L. LaConte, N. Nitin, and G. Bao, Magnetic nanoparticle probes. *Materials Today*, 2005, 8: 32-38.

[2] D. Patel, J.Y. Moon, Y. Chang, et al., Colloid surf, magnetic iron oxide nanoparticles: Synthesis and surface functionalization strategies. *Nanoscale Res Lett*, 2008, 3: 397-415.

[3] M. Zhao, L. Josephson, Y. Tang, et al., Magnetic sensors for protease assays. *Angewandte Chemie Intenational Edition*, 2003, 42: 1375.

[4] É.L. Freitas, C.F. Juliana, R.P. Rafael, et al., Magnetite content evaluation on magnetic drug delivery systems by spectrophotometry: A technical note. *AAPS Pharm. Sci. Tech.*, 2011, 12(2): 521-524.

[5] P.D. Stevens, J. Fan, H.M.R. Gardimalla, et al., Superparamagnetic nanoparticle-supported catalysis of Suzuki cross-coupling reactions. *Org Lett,* 2005, 7(11): 2085-2088.

[6] Y. Jun, J. Choi, and J. Cheon, Heterostructured magnetic nanoparticles: their versatility and high performance capabilities. *Chemical communications*, 2007: 1203-1214 .

[7] A.K. Gupta, M. Gupta, Synthesis and surface engineering of iron oxide nanoparticles for biomedical applications. *Biomaterials*, 2005, 26(18): 3995-4021.

[8] R.M. Cornell, U. Schwertmann, the Iron oxides: Structures, properties, reactions, occurences and uses. *Wiley-VCH*, *Weinheim*, 2003.

[9] W. Wu, Q. He, and C. Jiang, Magnetic iron oxide nanoparticles: Synthesis and surface functionalization strategies. *Nanoscale Res Lett*, 2008, 3(11): 397-415.

[10] S.R. Pandya, M. Singh, Preparation and characterization of magnetic nanoparticles and their impact on anticancer drug binding and release processes moderated through 1st tier dendrimer. *RSC Advances*, 2016.

[11] Government of India, Ministry of Health and Family Welfare, *Pharmacopoeia I.* vol. II. Delhi: The Controller of Publication, 1996, 634.

[12] X.N. Yang, I. Khan, and S.C. Kang, Chemical composition, mechanism of antibacterial action and antioxidant activity of leaf essential oil of Forsythia Korean deciduous shrub. *Asian Pacific Journal of Tropical Medicine*, 2015, 8: 694-700.

[13] R. Kockro, J. Hampl, B. Jansen, et al., Use of scanning electron microscopy to investigate the prophylactic efficacy of rifampin-impregnated CSF shunt catheters. *Journal of Medical Microbiology*, 2000, 49: 441-500.

[14] M.S. Jabir, G.M Suliman, Z.J. Taqi, et al., Iraqi propolis increases degradation of IL-1b and NLRC4 by autophagy following *Pseudomonas aeruginosa* infection. *Microbes and Infection*, 2018, 18: 89-100.

[15] C. Xu, Z. Wang, L. Wang, et al., Bias voltage-dependent low field spin transport properties of Fe_3O_4-PEG with different particle sizes. *Modern Physics Letters B*, 2016, 30(23): 1650301.

[16] I. Karimzadeh, H.R. Dizaji, and M. Aghazadeh, Preparation, characterization and PEGylation of superparamagnetic Fe_3O_4 nanoparticles from ethanol medium via cathodic electrochemical deposition (CED) method. *Materials Research Express*, 2016, 3: 095022.

[17] I. Karimzadeh, M. Aghazadeh, T. Doroudi, et al., Superparamagnetic iron oxide (Fe_3O_4) nanoparticles coated with PEG/PEI for biomedical applications: A facile and scalable preparation route based on the cathodic electrochemical deposition method. *Advances in Physical Chemistry*, 2017: Article ID 9437487, 7 pages.

[18] F. Ji, K. Zhang, J. Li, et al., A dual pH/magnetic responsive nanocarrier based on PEGylated Fe_3O_4 nanoparticles for doxorubicin delivery.*Journal of Nanoscience and Nanotechnology*, 2018,18: 4464-4470.

[19] B. Feng, R.Y. Hong, L.S. Wang, et al., Synthesis of Fe_3O_4/APTES/PEG diacid functionalized magnetic nanoparticles for MR imaging. *Colloids and Surfaces A: Physicochem. Eng. Aspects*, 2008, 328: 52-59.

[20] L. Sheikh, R. Vohra, A.K. Verma, et al., Biomimetically synthesized aqueous ferrofluids having antibacterial and anticancer properties. *Materials Sciences and Applications*, 2015, 6: 242-250.

[21] J.W. Park, K.H. Bae, C. Kim, et al. Clustered magnetite nanocrystals cross-linked with PEI for efficient siRNA delivery. *Biomacromolecules*, 2011, 12: 457-465.

[22] J. Lin, K. Nishino, M.C. Roberts, et al., Mechanisms of antibiotic resistance. *Front Microbiol,* 2015, 5(6): 34.

[23] J.H. Doughari, P.A. Ndakidemi, I.S. Human, et al., Antioxidant, antimicrobial and antiverotoxic potentials of extracts of Curtisia dentata. *Journal of Ethnopharmacol.,* 2012 ,141(3): 1041-1050.

[24] M.S. Jabir, T.A. Ali, and S.I. Usama, Linalool loaded on glutathione-modified goldnanoparticles: A drug delivery system for a successful antimicrobial therapy. *Artificial Cells, Nanomedicine, and Biotechnology*, 2018(2): 1-10.

[25] K.S. Khashan, M.S. Jabir, and F.A. Abdulameer, Carbon nanoparticles decorated with cupric oxide nanoparticles prepared by laser ablation in liquid as an antibacterial therapeutic agent. *Material Research Express*, 2018, 5(3): 035003.

[26] S.A. Mohamed, H.A. Nhung, A.S. Nguyen, et al., Functionalized magnetic nanoparticles and their effect on *Escherichia coli* and *Staphylococcus aureus*. *Journal of Nanomaterials*, 2015: Article ID 416012.

[27] M.H. Kim, I. Yamayoshi, S. Mathew, et al., Erratum to: Magnetic nanoparticle targeted hyperthermia of cutaneous *Staphylococcus aureus* infection. *Annals of Biomedical Engineering*, 2013, 41(3): 610.

Copyright© Majid Sakhi Jabir, Uday Muhsen Nayef, and Waleed Kamel Abdul Kadhim. This is an open-access article distributed under the terms of the Creative Commons Attribution License, which permits unrestricted use, distribution, and reproduction in any medium, provided the original author and source are credited.